

Circular Groove Guide for Short Millimeter and Submillimeter Waves

Hong-Sheng Yang, *Senior Member, IEEE*, Jianglei Ma, *Member, IEEE*, and Zhong-Zuo Lu

Abstract—A new type of groove guide, circular groove guide, has been designed for use as a low losses, high power handling, low dispersion and single mode transmission medium in the short millimetric and submillimetric waves ranges. The characteristic equations of TE modes and TM modes have been developed and the propagation characteristics of the fundamental mode have been discussed. Experimental measurements are in good agreement with theoretical results.

I. INTRODUCTION

IN ORDER TO develop the frequency spectrum from short millimeter to submillimeter waves, the search for efficient and powerful sources of coherent radiation is an active area in which solid-state IMPATT and Gunn devices, traditional and relativistic electron devices such as carcinotrons and gyrotrons etc. and optically pumped lasers have had extensive development. On the other hand people make strong efforts to develop new transmission medium for this part of the frequency spectrum. Many transmission guides have been developed. According to power level they can roughly be divided into two categories: one is of low power level and the other is of moderate or high power level. Now we pay more attention to the latter one. When the frequency is increased above 100 GHz, traditional rectangular wave guide is progressively more prohibitive, because the attenuation increases with frequency, the dimensions of guide are scaled down in proportion to the wavelength, the fabrication problems are severe with subsequent very high cost and the power handling capability is decreased. Oversized guide suffers from the generation and transmission of higher order modes produced at discontinuities. The TE_{01}^0 mode in circular guide has the characteristic of loss that decreases as the frequency increases, but it is not the dominant mode.

H guide and groove guide have the attractive features of large dimensions relative to the wavelength, single mode transmission, low dispersion, and a loss which is very low compared with that of rectangular guide. In H guide the presence of the dielectric bar results in the disadvantage of requiring a slot depth, the penetration of the dielectric bar into the conducting surface, with a dimension critical to a fraction of a wavelength and therefore of being frequency sensitive. Elimination of the dielectric bar in groove guide reduces the losses. Especially groove guide is simple to construct and has

Manuscript received September 22, 1993; revised May 18, 1994. This work was supported by the National Natural Science Foundation of P. R. China.

The authors are with the Department of Electronic Engineering, National Key Laboratory of Millimeter Waves, Southeast University, Nanjing 210018, The People's Republic of China.

IEEE Log Number 9407283.

a wider frequency range. For high power handling we prefer the groove guide to H guide.

The groove guide was first proposed by F. J. Tischer in 1952. [1] Ever since the field distribution and characteristics of groove guide have been analyzed by many authors. [2]–[5] Most of them deal with the groove guide with the cross section of rectangular groove or V -shape groove. Rectangular groove guide can be easily transformed to common rectangular waveguide which is used as output window of most active sources. However the developments of relativistic electron beam oscillators giving high power levels have completely changed the situation that all power sources at those frequency band were at low power levels. Recently, high power gyrotrons are readily available. They have seen application in fusion research and undoubtedly will soon see use in communications and radar. It is obvious that gyrotrons need a wave guide of low losses, high power handling, and dominant mode transmission.

Gyrotrons are based on the interaction between a relativistic electron beam and an electromagnetic field in an open resonator with circular cross-section. Consequently the authors have put forward a new type of groove guide—a circular groove guide [6]—which may be transformed to gyrotrons more conveniently than other ones.

This paper describes the fundamental characteristics of the circular groove guide. In Section II the characteristic equations of $TE_{pn}^{(r)}$ and $TM_{pn}^{(r)}$ modes will be derived. Based on these expressions the cutoff wavelength distribution of $TE_{pn}^{(r)}$ and $TM_{pn}^{(r)}$ modes is obtained in Section III. The propagation characteristics of dominant $TE_{11}^{(1)}$ mode are calculated in Section IV. The design method of circular groove guide and the experimental results are given in Sections V and VI, respectively. Experimental results agree with the theoretical calculations.

II. CHARACTERISTIC EQUATIONS

The structure of circular groove guide is shown in Fig. 1. It consists of two parallel conducting plates with spacing $2c$. At the symmetrical center of the transverse cross section there is a circular through hole along Z axis. The up and down ends are kept open or loaded with absorbent material.

It is assumed that the circular groove guide with uniform cross section extends to infinity in the Z direction which is the direction of wave propagation and the dielectric inside the guide is homogeneous. Then the cross section of circular groove guide is shown in Fig. 2. The guide can be divided

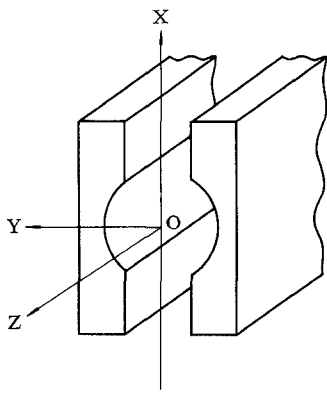


Fig. 1. The structure of circular groove guide.

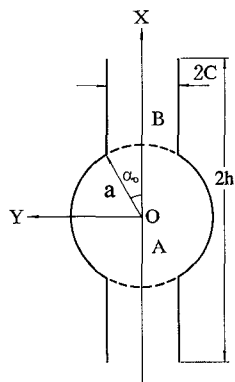


Fig. 2. The cross section of circular groove guide.

into three parts, i.e. the central groove region designated by *A* which has circular boundary with diameter $2a$ and two evanescent side regions designated by *B*. According to that geometrical shape, we take cylindrical coordinates in region *A* and rectangular coordinates in region *B*. They have the same *Z* axis.

There are two types of modes existing in circular groove guide, i.e., TE modes and TM modes. To distinguish different modes, the symbols $TE_{pn}^{(r)}$ and $TM_{pn}^{(r)}$ are used to represent TE modes and TM modes of different order respectively, where r , p , n are integers. Superscript r denotes the number of half waves of electric or magnetic intensity in the *Y* direction in parallel plate region, and subscript p refers to the number of cyclic variations with α and n represents the n th root of the Bessel function and it is a measure of the radial variation of the field pattern in circular groove guide.

A. The First-Order Approximate Characteristic Equation of $TE_{pn}^{(r)}$ Mode

In circular groove guide, energy is mainly confined in central circular groove region provided the spacing between two parallel plates is not very large. Under this condition the field distribution in circular groove region is similar to that in circular waveguide but the polarization degeneracy is eliminated. Besides, there is some leaking energy in parallel plate region. For the mode which can transmit along *Z* direction,

the field in region *B* must be exponentially evanescent in *X* direction.

The longitudinal field components of $TE_{pn}^{(r)}$ mode under first-order approximation can be expressed as follows:

$$\begin{cases} \dot{H}_{zA} = H_p J_p(k_c \rho) \sin p\alpha & \text{(region } A\text{)} \\ \dot{H}_{zB} = B_r k_c^2 \sin\left(\frac{r\pi y}{2c}\right) \exp[-k_{xr}(x - x_0)] & \text{(region } B\text{)} \end{cases} \quad (1)$$

where $p = 1, 2, 3, \dots$; $r = 1, 3, \dots$; k_c is cutoff wavenumber; jk_{xr} and $k_{yr} = \frac{r\pi}{2c}$ are the wavenumbers in *X* and *Y* direction respectively in region *B*; J_p is *p*-order Bessel function; H_p and B_r are the amplitude coefficients in region *A* and region *B* separately and x_0 is the scale value of *x* coordinate at the arc boundary between region *A* and *B*.

The transverse components of the field can be derived from Maxwell equations:

Region *A*:

$$\begin{aligned} \dot{E}_{\rho A} &= -j \frac{\omega \mu_0}{k_c^2} \frac{H_p}{\rho} p J_p(k_c \rho) \cos p\alpha \\ \dot{E}_{\alpha A} &= j \frac{\omega \mu_0}{k_c} H_p J'_p(k_c \rho) \sin p\alpha \\ \dot{H}_{\rho A} &= -j \frac{\beta}{k_c} H_p J'_p(k_c \rho) \sin p\alpha \\ \dot{H}_{\alpha A} &= -j \frac{\beta}{k_c^2} \frac{H_p}{\rho} p J_p(k_c \rho) \cos p\alpha. \end{aligned} \quad (2)$$

Region *B*:

$$\begin{aligned} \dot{E}_{x B} &= -j \omega \mu_0 B_r k_{yr} \cos(k_{yr} y) \exp[-k_{xr}(x - x_0)] \\ \dot{E}_{y B} &= -j \omega \mu_0 B_r k_{xr} \sin(k_{yr} y) \exp[-k_{xr}(x - x_0)] \\ \dot{H}_{x B} &= j \beta B_r k_{xr} \sin(k_{yr} y) \exp[-k_{xr}(x - x_0)] \\ \dot{H}_{y B} &= -j \beta B_r k_{yr} \cos(k_{yr} y) \exp[-k_{xr}(x - x_0)]. \end{aligned}$$

The boundary conditions between region *A* and *B* are given by following expression:

$$\begin{cases} \dot{H}_{zA} = \dot{H}_{zB} & (\rho = a, 0 \leq \alpha \leq \alpha_0) \\ \dot{E}_{\alpha A} = \begin{cases} E_{\alpha B} & (\rho = a, 0 \leq \alpha \leq \alpha_0) \\ 0 & (\rho = a, \alpha_0 \leq \alpha \leq \frac{\pi}{2}) \end{cases} & \end{cases} \quad (3)$$

By making use of field components (1), (2) and boundary conditions (3), following characteristic equation of $TE_{pn}^{(r)}$ mode is obtained.

$$\frac{u J'_p(u)}{J_p(u)} = \frac{8a A_1(p, r)[r M A_2(p, r) - \nu(r) A_1(p, r)]}{\pi c}. \quad (4)$$

There is another relation between unknowns u and $\nu(r)$.

$$u^2 = (rM)^2 - \nu^2(r) \quad (5)$$

where

$$A_1(p, r) = \int_0^{\alpha_0} \sin p\alpha \sin(rM \sin \alpha) \cos \alpha d\alpha$$

$$A_2(p, r) = \int_0^{\alpha_0} \sin p\alpha \cos(rM \sin \alpha) \sin \alpha d\alpha$$

$$u = k_c a, \quad \nu(r) = k_{xr} a, \text{ and } M = \frac{\pi a}{2c}.$$

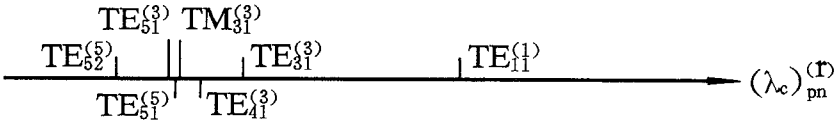


Fig. 3. The diagram of cutoff wavelength of circular groove guide ($\frac{2c}{2a} = 0.65$).

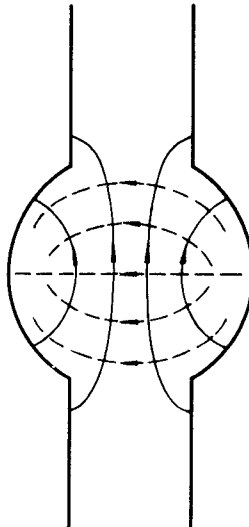


Fig. 4. Distribution of the transverse components of the field of $TE_{11}^{(1)}$ mode. — electric field; - - - magnetic field.

B. The First-Order Approximate Characteristic Equation of $TM_{pn}^{(r)}$ Mode

The longitudinal field components of $TM_{pn}^{(r)}$ mode are \dot{E}_z . Following expression gives the \dot{E}_z components of $TM_{pn}^{(r)}$ mode in two different regions.

$$\begin{cases} \dot{E}_{zA} = H_p J_p(k_c \rho) \cos p\alpha & \text{(region A)} \\ \dot{E}_{zB} = B_r k_c^2 \cos\left(\frac{r\pi y}{2c}\right) \exp[-k_{xr}(x - x_0)] & \text{(region B).} \end{cases} \quad (6)$$

The transverse components of the fields for TM modes can be derived from Maxwell equations also. The boundary condition for TM modes is different from that of TE modes. It is written below.

$$\begin{cases} \dot{E}_{zA} = \begin{cases} \dot{E}_{zB} & (\rho = a, 0 \leq \alpha \leq \alpha_0) \\ 0 & (\rho = a, \alpha_0 \leq \alpha \leq \frac{\pi}{2}) \end{cases} \\ \dot{H}_{\alpha A} = \dot{H}_{\alpha B} \quad (\rho = a, 0 \leq \alpha \leq \alpha_0). \end{cases} \quad (7)$$

Let:

$$\begin{aligned} E_1(p, r) &= \int_0^{\alpha_0} \cos(rM \sin \alpha) \cos p\alpha d\alpha \\ E_2(r_1, r_2) &= \int_0^{\alpha_0} \sin(r_1 M \sin \alpha) \cos(r_2 M \sin \alpha) \sin \alpha \cos \alpha d\alpha \\ E_3(r_1, r_2) &= \int_0^{\alpha_0} \cos(r_1 M \sin \alpha) \cos(r_2 M \sin \alpha) \cos^2 \alpha d\alpha \\ E_4(p, r) &= \int_0^{\alpha_0} \cos(rM \sin \alpha) \cos p\alpha \cos \alpha d\alpha. \end{aligned}$$

Then we can derive the characteristic equation of $TM_{pn}^{(r)}$ mode

$$\frac{u J'_p(u)}{J_p(u)} = -\frac{\pi[rM E_2(r_1, r_2) + \nu(r) E_3(r_1, r_2)]}{4E_1(p, r) E_4(p, r)}. \quad (8)$$

III. THE CUTOFF WAVELENGTH DISTRIBUTION OF $TE_{pn}^{(r)}$ AND $TM_{pn}^{(r)}$ MODES IN CIRCULAR GROOVE GUIDE

The general expressions of characteristic equation (4) and (8) for $TE_{pn}^{(r)}$ mode and $TM_{pn}^{(r)}$ mode have been derived. The solutions of the characteristic equations for $TE_{pn}^{(r)}$ and $TM_{pn}^{(r)}$ mode are obtained by solving simultaneous equations (4) and (5) as well as (8) and (5). From the relation $\lambda_c = \frac{2\pi a}{u_{pn}^{(r)}}$ the cutoff wavelengths of the modes in circular groove guide can be calculated.

In order to ensure that the energy transmits along Z direction in circular groove guide, the field must be evanescent in X direction. This requires that k_{xr} is real. $\nu^2(r) > 0$ means that k_{xr} is real and corresponds to transmitting mode in z direction, while $\nu^2(r) < 0$ expresses nontransmitting mode. From expression (5), we know that $\nu^2(r)$ is relevant to parameter $\frac{2c}{2a}$ and the order number p, n, r . Therefore some higher order modes can be suppressed under certain waveguide dimensions. If $\frac{2c}{2a} > 0.6$, only $TE_{11}^{(1)}$, $TE_{31}^{(3)}$, $TE_{41}^{(3)}$, $TE_{51}^{(5)}$, $TE_{52}^{(5)}$ and $TM_{31}^{(3)}$ modes can transmit along Z direction and other modes become not transmissible. Fig. 3 gives the distribution of cutoff wavelengths of these modes.

From Fig. 3, it is obvious that the mode $TE_{11}^{(1)}$ has the longest cutoff wavelength (lowest cutoff frequency) in the circular groove guide and is called dominant mode. The field distribution of $TE_{11}^{(1)}$ mode is shown in Fig. 4.

IV. DOMINANT MODE $TE_{11}^{(1)}$ AND PROPAGATION CHARACTERISTICS

Among all of the possible modes, $TE_{11}^{(1)}$ mode is the dominant mode and the other modes corresponding to $p > 1$, $n > 1$ or $r > 1$ are all higher-order mode. These modes are further divided into odd-order modes and even-order modes depending on whether p is odd or even. However, only the $TE_{pn}^{(r)}$ mode family, in which p is odd, has valuable and interesting properties. Especially we pay more attention to the dominant mode $TE_{11}^{(1)}$.

A. The Second-Order Approximate Characteristic Equation of $TE_{11}^{(1)}$ Mode

In order to get precise expression of characteristic equation, we should use infinite series to describe the field components in circular groove guide. For $TE_{11}^{(1)}$ mode, expressions are as follows:

$$\begin{cases} \dot{H}_{zA} = \sum_p H_p J_p(k_c \rho) \sin p\alpha & \text{(region A)} \\ \dot{H}_{zB} = \sum_r B_r k_c^2 \sin\left(\frac{r\pi y}{2c}\right) \exp[-k_{xr}(x - x_0)] & \text{(region B)} \end{cases} \quad (9)$$

where $p = r = 1, 3, 5, \dots$

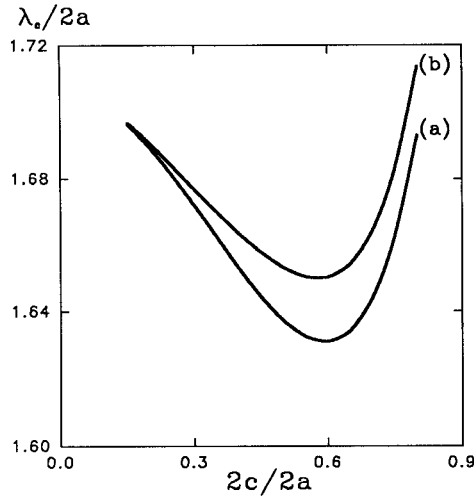


Fig. 5. The relation between $\frac{\lambda_c}{2a}$ and $\frac{2c}{2a}$. (a) First-order approximation. (b) Second-order approximation.

Theoretically, the precise solution can be obtained if the field components in circular groove guide are expressed by infinite series as expression (9). But in practical analyses, only limited terms are taken and the solution is approximate.

If p and r are taken by both 1 and 3, the second-order approximate characteristic equation of $TE_{11}^{(1)}$ mode is derived.

$$\frac{(uJ'_1(u)/J_1(u)) + t_1}{t_2} = \frac{t_3}{t_4 - (uJ'_3(u)/J_3(u))} \quad (10)$$

where

$$t_1 = K[R(1, 1)S_3 - R(1, 3)S_1]$$

$$t_2 = K[R(1, 3)S_2 - R(1, 1)S_4]$$

$$t_3 = K[R(3, 1)S_3 - R(3, 3)S_1]$$

$$t_4 = K[R(3, 3)S_2 - R(3, 1)S_4]$$

$$K = -\frac{16a^2}{\pi c^2}$$

$$S_1 = -\frac{c}{2a}A_1(1, 3)$$

$$S_2 = -\frac{c}{2a}A_1(3, 3)$$

$$S_3 = \frac{c}{2a}A_1(1, 1)$$

$$S_4 = \frac{c}{2a}A_1(3, 1)$$

$$R(p, r) = rMA_2(p, r) - \nu(r)A_1(p, r).$$

B. Cutoff Wavelength

Fig. 5 shows the relation between $\frac{\lambda_c}{2a}$ of $TE_{11}^{(1)}$ mode and normalized plate spacing $\frac{2c}{2a}$. The varying tendency of the curves coincides with the theoretical result of rectangular groove guide given by A. A. Oliner [3]. It can also be seen from Fig. 5 that the two ends of the curves approach to 1.7 and 2 respectively. The former is the corresponding value of lowest mode in circular waveguide and the later is that for lowest mode in parallel plate guide. The variation of $\frac{P_A}{(P_A+P_B)}$ with normalized plate spacing $\frac{2c}{2a}$ is shown in Fig. 6, where P_A and P_B are the powers transmitting in region (A) and (B) respectively. With the increment of $\frac{2c}{2a}$ from zero to 1, the

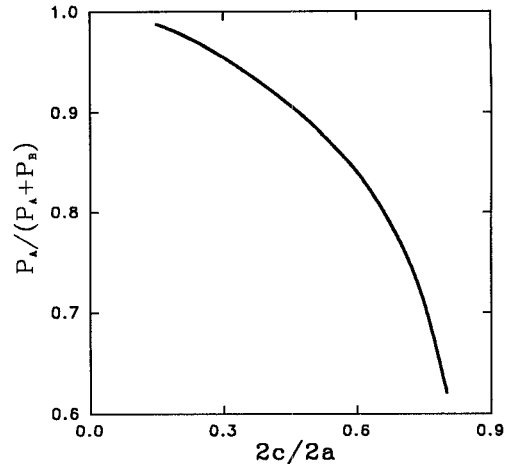


Fig. 6. The variation of $\frac{P_A}{(P_A+P_B)}$ with $\frac{2c}{2a}$.

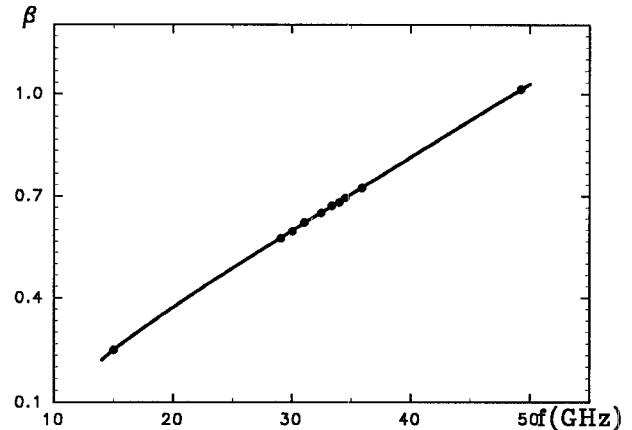


Fig. 7. The dispersion curve of circular groove guide • Experiment-Theory.

ratio $\frac{P_A}{(P_A+P_B)}$ drops monotonously. It means that when groove guide is changing to parallel plate guide, its ability to confine energy in central circular groove region is becoming weak.

C. Propagation Constant and Dispersion Property

With the help of formula $\frac{2\pi f}{\beta} = \frac{c}{\sqrt{1-(\lambda/\lambda_c)^2}}$ and the cutoff wavelengths obtained above, we have the dispersion curve. Fig. 7 gives the theoretical relation of phase constant β and operating frequency f . From this figure, we find that as expected the dispersion curve is almost straight line. It means that the dispersion of circular groove guide is very low.

D. Attenuation Coefficient

The loss in circular groove guide can be readily computed when the eigenvalue of characteristic equation for $TE_{11}^{(1)}$ mode is known. Here, copper and aluminum are chosen as guide material. Fig. 8 shows the attenuation curve. The curve suggests that the attenuation constant of circular groove guide is about an order of magnitude less than that of dominant TE_{10} mode of rectangular waveguide. Fig. 9 gives the relation between attenuation constant α of circular groove guide and the normalized plane separation $\frac{2c}{2a}$. The curve indicates that the attenuation constant becomes less when the plane separation

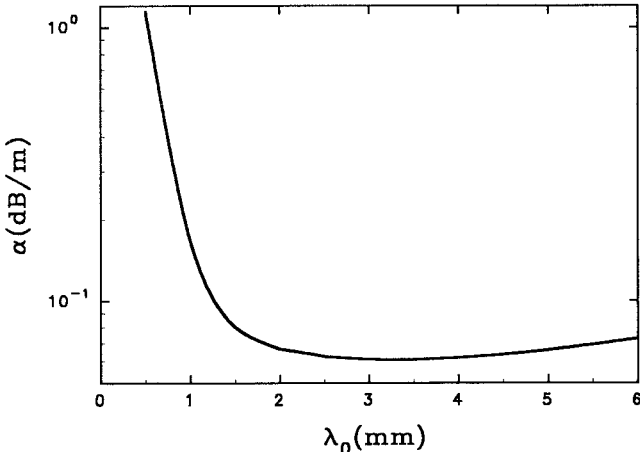


Fig. 8. Circular groove guide attenuation ($2a = 10$ mm, $\frac{2c}{2a} = 0.7$, copper).

becomes larger. The change of $\frac{2c}{2a}$ from zero to 1 corresponds to the transition from circular waveguide to circular groove guide and then to parallel plate guide. When the parallel plate guide is excited by TE mode, the loss is very low because the electric field vector is parallel to the metallic walls. The larger the plane separation of the groove guide, the more similar it to parallel plate guide, and therefore the corresponding attenuation constant becomes less of course. Besides, the variation of radiation attenuation constant α_R with the height of parallel plate region is also investigated in Fig. 10. The radiation loss decreases when h/λ increases, where $2h$ is the height of the guide. This is because the increment of the height of the parallel plate causes the reduction of the power leaking out from the guide edges.

V. DESIGN OF CIRCULAR GROOVE GUIDE

The single mode operation range of circular groove guide can be determined from Fig. 3. It is $1.47a < \lambda_0 < 3.27a$ or $0.31\lambda_0 < a < 0.68\lambda_0$. Compared with circular waveguide, the dimension of single mode operation is larger and the frequency range is broader. In circular groove guide, only TE odd-order modes has the low loss characteristics, while TE even-order modes and TM modes do not have this advantage. So in practical application, we must use TE wave to excite the guide and restrain TE even modes as far as possible. Besides, when the relative parallel plate spacing $\frac{2c}{2a}$ is taken as 0.65, the mode order number in y direction in region B must satisfy $r < 3$. So it can be considered that under this condition TE₃₁⁽³⁾ mode is not existent. By virtue of above consideration, the single mode operation range can be further broadened. In our design the single mode dimensions of circular groove guide is chosen as follow: $\frac{2c}{2a}$ is around 0.65 and the radius of circular groove satisfies:

$$0.31\lambda_0 < a < 1.01\lambda_0 \quad (11)$$

It suggests that radius of circular groove under single mode operation can be twice as much as that of circular waveguide and that the operating frequency range is also much larger than that of circular waveguide. According to Fig. 10, it is needed that the height of parallel plate region h is larger than 5λ .

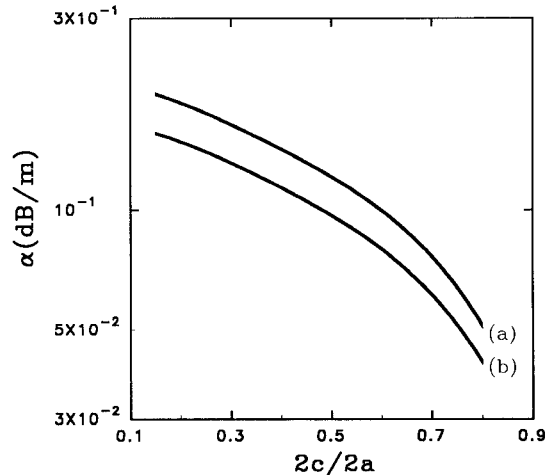


Fig. 9. The relation between attenuation constant α and normalized plane separation $\frac{2c}{2a}$ (a) aluminum; (b) copper.

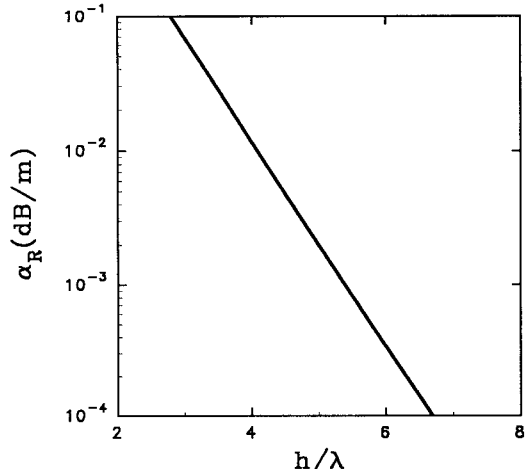


Fig. 10. The variation of α_R with h/λ .

VI. EXPERIMENTAL MEASUREMENTS

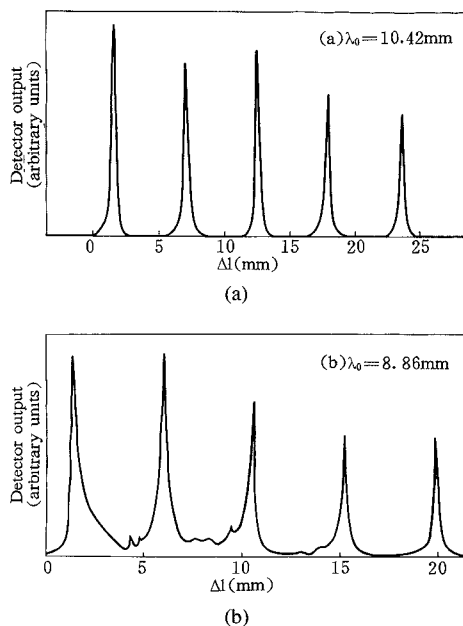
Some experimental measurements have been made at V , Q and K bands to verify our theoretical results. The resonant technique is used to determine the guide wavelength and moding spectrum.

In our measuring systems, the sources were reflex klystrons which operate at the V , Q and K bands. The waveguide resonator was formed by a length of circular groove guide under test terminated at one end by a fixed conducting plate with an input aperture and at the other end by non-contacting sliding short-circuit plunger with an output aperture on which a crystal detector was mounted. By continuously varying the length of waveguide resonator, the resonance spectrum was obtained, from which the guide wavelength could be determined according to resonance peak separation and the moding characteristics were known on the basis of overall pattern.

The measured guides of two different dimensions were constructed from aluminium plate by conventional workshop techniques. Measurements were made at V , Q , and K bands respectively.

TABLE I
GUIDE WAVELENGTHS

Operating Wavelength λ_0 (mm)	Guide Wavelengths λ_g (mm)		$\frac{ \lambda_{g2} - \lambda_{g1} }{\lambda_{g2}} \times 100$ (%)
	Experimental results (λ_{g1})	Theoretical Calculations (λ_{g2})	
6.09*	6.188	6.199	0.2
8.86*	9.196	9.208	0.1
19.93**	21.016	20.982	0.2

* Guide dimensions: $2c = 13\text{mm}$, $2a = 20\text{mm}$, $2h = 140\text{mm}$ ** Guide dimensions: $2c = 26\text{mm}$, $2a = 38.9\text{mm}$, $2h = 200\text{mm}$ Fig. 11. Moding spectrum for circular groove guide cavity of variable length (guide dimensions $2c = 13\text{ mm}$, $2a = 20\text{ mm}$, $2h = 140\text{ mm}$). (a) $\lambda_0 = 10.42\text{ mm}$. (b) $\lambda_0 = 8.86\text{ mm}$.

The experimental and theoretical guide wavelengths λ_g of the guides under test are given in Table I. The guide wavelengths λ_{g1} and λ_{g2} are close to each other.

The dispersion curve of circular groove guide was also verified by experiment. The measurement data marked by points are shown in Fig. 7 too. The correlation between theoretical and experimental results is very good indeed.

Fig. 11 gives the measured moding spectra for certain guide dimensions at different operating wavelengths, in which (a) corresponds to single mode transmitting and (b) indicates the higher-order modes' existing. In situation (a) the ratio of the radius of circular groove to operating wavelength $\frac{a}{\lambda_0}$ is 0.96 and lies in the single mode operating range given in section V, but in situation (b) the value of $\frac{a}{\lambda_0}$ is 1.13 and is beyond this range. This fact demonstrates that the single mode operating range predicted from theoretical equation (11) is reasonable.

VII. CONCLUSION

Circular groove guide has been studied theoretically and experimentally. In the theoretical analyses, the first order approximate characteristic equation of $\text{TE}_{pn}^{(r)}$ and $\text{TM}_{pn}^{(r)}$ modes and second order approximate characteristic equation of the dominant mode in circular groove guide have been derived. The cutoff wavelength distribution has been researched and the condition for single mode propagation has been given. The parameters of $\text{TE}_{11}^{(1)}$ mode such as cutoff wavelength and guide wavelength, have been obtained by computer calculation, the attenuation characteristics and the dispersion property have been analyzed. In the experimental measurements, the resonant curves have been measured at V , Q and K bands respectively. From these curves, the guide wavelengths, dispersion relation and moding characteristics can be determined. Experimental results are in good agreement with theoretical calculations.

The study shows that with proper choice of guide dimension, circular groove guide has advantages of low loss, low dispersion, large dimensions, single mode operating and high power handling capacity. Besides, it is easy to manufacture and connect. The frequency band of circular groove guide is relatively broad. Therefore, circular groove guide is a comparatively ideal transmission medium for short millimeter wave and submillimeter wave, particularly under high-power condition.

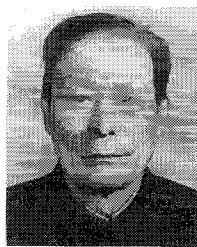
REFERENCES

- [1] F. A. Benson and F. J. Tischer, "Some guiding structures for millimeter waves," *IEEE Proc.* vol. 131, pt. A, no. 7, pp. 429-449.
- [2] Yat Man Choi and D. J. Harris, "Groove guide for short millimetric waveguide systems," *Infrared and Millimeter Waves*, vol. 11, pp. 99-140.
- [3] A. A. Oliner and Paolo Lampariello, "The dominant mode properties of open groove guide: an improved solution," *IEEE Trans. Microwave Theory Tech.* vol. MTT-33, no. 9, 1985, pp. 755-764.
- [4] T. Nakahara and N. Kurauchi, "Transmission modes in the grooved guide," *J. Inst. Electron. Commun. Eng. Jap.*, vol. 47, no. 7, pp. 43-51, July 1964.
- [5] Y. M. Choi and D. J. Harris, "Theoretical and experimental characteristic of single v-groove guide for X-band and 100 GHz operation," *IEEE Trans. Microwave Theory Tech.*, vol. MTT-36, no. 4, 1988, pp. 715-722.
- [6] Yang Hong-Sheng, Ma Jianglei, and Lu Zhong-Zuo, "A new type of groove guide," in *2nd Int. Symp. Recent Advances in Microwave Tech.*, 1989, pp. 239-240.



Hong-Sheng Yang (SM'94) was born in Zhejiang Province, China, on January 21, 1938. He graduated from Nanjing Institute of Technology, Nanjing, China, in 1962.

Since 1962, he has been a faculty member of the Electronic Engineering Department, Nanjing Institute of Technology, now Southeast University. He has taught undergraduate and graduate courses and done research work in the fields of electromagnetic theory, microwave and millimeter wave technique and devices. From March 1981 to September 1983, he was a visiting scholar and research associate in the Department of Electrical and Computer Engineering at University of Wisconsin, Madison, where he engaged in research on using high power lever millimeter wave generated by gyrotron for heating plasma in thermonuclear reactor by mode transducing antenna. He is now a professor and a director of the Microwave and Millimeter Wave Electronics Division in the Department of Electronic Engineering. He joined the National Key Laboratory of Millimeter Waves in 1991. His current interests are shortmillimeter and submillimeter wave electronics and techniques. He is the co-author of the textbook *Millimeter Wave Techniques and Devices* (Southeast University Press, 1991) and the dictionary *Modern Electron Science and Technology Dictionary* (Electronics Industry Press, 1992).



Zhong-Zuo Lu was born in Jiangsu Province, China, on November 24, 1913. He received the B.S.E.E. degree from the National Central University, China, in 1938 and the M.S. degree from the University of Michigan, Ann Arbor, in 1946.

From 1938 to 1945 he was employed as an associate engineer by Kunming factory of National Central Radio Manufacturing Factory. From 1946 to 1947 he was a visiting engineer at Marconi and RCA Company in Canada. At the end of 1947 he was a director of research division of Nanjing factory in National Central Radio Equipment Company of China. He joined the National Central University, Nanjing, as an associate professor in 1948. From 1949 to 1952 he was with Nanjing University. Since 1952 he has been with Nanjing Institute of Technology, now Southeast University, first with its Department of Radio Engineering where he holds the position of professor and vicechairman of the Department and presently with its Department of Electronic Engineering and Research Institute of Electronics. Between 1963 to 1985 he was appointed head in that Department and Institute, where he was engaged in research on microwave and millimeter wave tubes and put forward a new design method of travelling wave tubes and carcinotrons. His current research interests are in the areas of microwave and millimeter wave electronics and techniques. He wrote five books, among them: *Microwave Techniques* (Beijing, Posts and Telecommunications Press, 1958), *Microwave Tubes* (Beijing, Posts and Telecommunications Press, 1958), *Travelling Wave Tubes* (Shanghai, Science Press, 1962).

In 1991 Professor Lu was nominated in The International Directory of Distinguished Leadership by ABI.



Janglei Ma (S'92-M'93) was born in Jiangsu Province, China, on June 3, 1961. She received the B.E. degree and M.E. degree from Nanjing Institute of Technology, now Southeast University, in 1982 and 1985 respectively and the Ph.D. degree from Southeast University in 1992.

In 1985, she joined the Electronic Engineering Department at Nanjing Institute of Technology and since then she has been engaged in educational activities for undergraduate and graduate students involving mathematic method in physics and electromagnetic field theory. Her research work has been related to dye laser, Raman spectrum, and guiding structure of short millimeter waves. She is presently associate professor in the Department of Electronic Engineering. Her current research is in the field of short millimeter and submillimeter wave techniques.